Mutation in the Monocarboxylate Transporter 12 Gene Affects Guanidinoacetate Excretion but Does Not Cause Glucosuria

Nasser Dhayat,*† Alexandre Simonin,‡§ Manuel Anderegg,*†‡§ Ganesh Pathare,*†‡§ Benjamin P Lüscher,†§‖ Christine Deisl,*†‡§ Giuseppe Albano,*†‡§ David Mordasini,*† Matthias A. Hediger,‡§‖ Daniel V. Surbek,†§‖ Bruno Vogt,*† Jörn Oliver Sass,¶** Barbara Kloeckener-Gruissem,††‡‡ and Daniel G. Fuster*†‡§

*Division of Nephrology, Hypertension and Clinical Pharmacology, and ‖Department of Obstetrics and Gynecology, University Hospital of Bern, Switzerland; ‡Institute of Biochemistry and Molecular Medicine, §Swiss National Centre of Competence in Research Transcure, and †Department of Clinical Research, University of Bern, Switzerland; ¶Division of Clinical Chemistry and Biochemistry, Children's Research Center, University Children's Hospital, Zürich, Switzerland; **Department of Natural Sciences, Bonn-Rhein-Sieg University of Applied Sciences, Rheinbach, Germany; ††Institute of Medical Molecular Genetics, University of Zürich, Zürich, Switzerland; and ‡‡Department of Biology, Swiss Federal Institute of Technology in Zürich, Zürich, Switzerland

ABSTRACT

A heterozygous mutation (c.643C>A; p.Q215X) in the monocarboxylate transporter 12-encoding gene *MCT12* (also known as *SLC16A12*) that mediates creatine transport was recently identified as the cause of a syndrome with juvenile cataracts, microcornea, and glucosuria in a single family. Whereas the *MCT12* mutation cosegregated with the eye phenotype, poor correlation with the glucosuria phenotype did not support a pathogenic role of the mutation in the kidney. Here, we examined MCT12 in the kidney and found that it resides on basolateral membranes of proximal tubules. Patients with *MCT12* mutation exhibited reduced plasma levels and increased fractional excretion of guanidinoacetate, but normal creatine levels, suggesting that MCT12 may function as a guanidinoacetate transporter *in vivo*. However, functional studies in *Xenopus* oocytes revealed that MCT12 transports creatine but not its precursor, guanidinoacetate. Genetic analysis revealed a separate, undescribed heterozygous mutation (c.265G>A; p.A89T) in the sodium/glucose cotransporter 2-encoding gene *SGLT2* (also known as *SLC5A2*) in the family that segregated with the renal glucosuria phenotype. When overexpressed in HEK293 cells, the mutant SGLT2 transporter did not efficiently translocate to the plasma membrane, and displayed greatly reduced transport activity. In summary, our data indicate that MCT12 functions as a basolateral exit pathway for creatine in the proximal tubule. Heterozygous mutation of *MCT12* affects systemic levels and renal handling of guanidinoacetate, possibly through an indirect mechanism. Furthermore, our data reveal a digenic syndrome in the index family, with simultaneous *MCT12* and *SGLT2* mutation. Thus, glucosuria is not part of the *MCT12* mutation syndrome.

J Am Soc Nephrol 27: 1426–1436, 2016. doi: 10.1681/ASN.2015040411

In 2007, Vandekerckhove *et al.* described a Swiss family with a unique, hitherto unknown syndrome consisting of juvenile cataract, microcornea, and renal glucosuria.[1] The mode of transmission was compatible with an autosomal-dominant trait. This initial description of the family did not include analysis of blood and urinary parameters of affected family members, and glucosuria was only mentioned qualitatively as present or absent. Interestingly, there was not a perfect concordance of the eye and kidney phenotype.

By a positional cloning approach, Kloeckener-Gruissem *et al.* identified a heterozygous nonsense mutation (c.643C>A; p.Q215×) in exon 6 of

Received April 16, 2015. Accepted August 5, 2015.

Published online ahead of print. Publication date available at www.jasn.org.

Correspondence: Dr. Daniel G. Fuster, Division of Nephrology, Hypertension and Clinical Pharmacology, University Hospital of Bern, Freiburgstrasse 15, 3010 Bern, Switzerland. Email: Daniel.Fuster@insel.ch

monocarboxylate transporter 12 gene *MCT12* (also known as *SLC16A12*), coding for MCT12, in affected family members.[2] Mutant p.Q215× MCT12 was predicted to encode a nonfunctional protein with only the first six of 12 transmembrane domains. When expressed in HEK293 cells, p.Q215× MCT12 was retained in the endoplasmatic reticulum (ER), while full-length MCT12 trafficked to the plasma membrane.[3] Surprisingly, *mct12* knockout (KO) rats did not display cataracts nor the glucosuria observed in family members with the heterozygous *MCT12* mutation.[3] Thus, the dominant form of cataract observed in the family was suspected to be due to protein misfolding, rather than haploinsufficiency.[3] Absence of glucosuria in *mct12* KO rats, and poor correlation of the *MCT12* mutation with the glucosuria trait in humans, suggested a dominant negative effect with incomplete penetrance or the presence of a second, independent mutation as the cause for the glucosuria observed in the family.[3]

The substrate of MCT12 was unknown until recently, when Abplanalp *et al.* deorphanized the transporter by use of an elegant metabolomics approach in *Xenopus laevis* oocytes.[4] MCT12 was found to be a Na^+- and Cl^-- independent creatine transporter. In support of these findings, *mct12* KO rats exhibited more than three-fold increased urinary excretion of creatine.[4]

Creatine and creatine-P act as spatial and temporal energy buffers in cells. Due to the spontaneous and irreversible conversion of creatine and creatine-P to creatinine (approximately 2% of the body's total creatine pool per day), there is a constant need for creatine replacement in the body.[5] Both biosynthesis and dietary intake maintain the creatine pool in humans. *De novo* creatine synthesis involves two enzymes, L-arginine:glycine amidinotransferase (AGAT) and guanidinoacetate methyltransferase (GAMT). AGAT catalyzes the transfer of a guanidine group from arginine to glycine to form ornithine and guanidinoacetate. GAMT catalyzes the transfer of a methyl group from S-adenosylmethionine to guanidinoacetate to form creatine and S-adenosylhomocysteine. Regulation of creatine biosynthesis occurs at the level of AGAT, and increased creatine levels lower AGAT enzyme activity.[6] High AGAT activity is found in the kidney, but AGAT activity has also been reported in other tissues, including the pancreas, brain, spleen, and testes.[5] In the kidney, guanidinoacetate is synthesized exclusively in the proximal tubule.[7] Renal production of the creatine precursor guanidinoacetate represents about 20% of the daily loss of creatine in humans, indicating that guanidinoacetate must also be synthesized at extrarenal sites.[8] The liver has no AGAT but high GAMT activity. Thus, creatine biosynthesis is an interorgan process, whereby guanidinoacetate produced by the kidney (and other sites) is released into circulation and methylated to creatine by the liver. In cells devoid of creatine biosynthesis, cellular uptake is achieved by the Na^+- and Cl^--dependent creatine transporter CRT1, encoded by *CRT1* (also known as *SLC6A8*). Mutation in *CRT1* leads to an X-linked cellular creatine-deficiency syndrome with mental retardation, increased plasma and urinary creatine levels, and resistance to creatine supplementation.[9,10] Blood and urine levels of the creatine precursor guanidinoacetate are normal in patients with *CRT1* mutations.

Patients with a heterozygous *MCT12* mutation do not display mental retardation, but have juvenile cataracts, microcornea, and glucosuria.[1,2] Creatine metabolism in humans with the heterozygous *MCT12* mutation has not been studied thus far. In addition, how heterozygous loss of the creatine transporter MCT12 could be causal to glucosuria remains poorly understood. To shed some light on the physiologic role of MCT12, we undertook a detailed phenotypic investigation of the Swiss index family and performed complementary *in vitro* studies.[1]

RESULTS

While renal expression of MCT12 has been reported previously, its tubular expression pattern has not been studied thus far.[2,3] To determine the distribution of MCT12 and CRT1 along the nephron, we isolated tubular segments by microdissection and quantified mRNA expression by RT-PCR (Figure 1). MCT12 transcripts are present in all segments but exhibit a four- to five-fold higher expression in proximal convoluted and proximal straight tubules, as well as thick ascending limbs of the loop of Henle, compared with those detected in the more distal segments, including distal convoluted tubules, connecting tubules, and cortical collecting ducts. Expression of CRT1 revealed a pattern similar to the one observed for MCT12, however, with an attenuated proximal-distal gradient (Figure 1).

We next also performed an expression analysis of both creatine transporters CRT1 and MCT12 in murine tissues by quantitative PCR (Supplemental Figure 1). These data reveal that the *MCT12* transcript is highly abundant in the lung, liver, kidney, and pancreas. In contrast, the highest transcript levels of *CRT1* are found in the epithelia of the gastrointestinal tract, followed by the brain, heart, lung, and kidney.

To define the subcellular localization of MCT12, we performed immunostaining and confocal imaging of murine kidney sections and isolated mouse proximal tubules with a previously validated MCT12 antibody.[3] As shown in Figure 2, A and B, the results suggest that MCT12 concentrates at the basolateral membrane. To further ascertain the subcellular localization of MCT12, we performed immunoblotting of total kidney membrane protein and brush border membrane protein preparations separated by SDS-PAGE (Figure 2C). Sodium/hydrogen exchanger isoform 1 (NHE1) and sodium/phosphate cotransporter isoform 2a (NaPi-2a) were used as typical representatives of basolateral and apical proximal tubular membrane proteins, respectively. The results indicate that MCT12 is not a brush border membrane protein (Figure 2C).

To obtain insights into the functional role of MCT12 in humans, we invited members of the original family to participate in a thorough phenotypic characterization. This

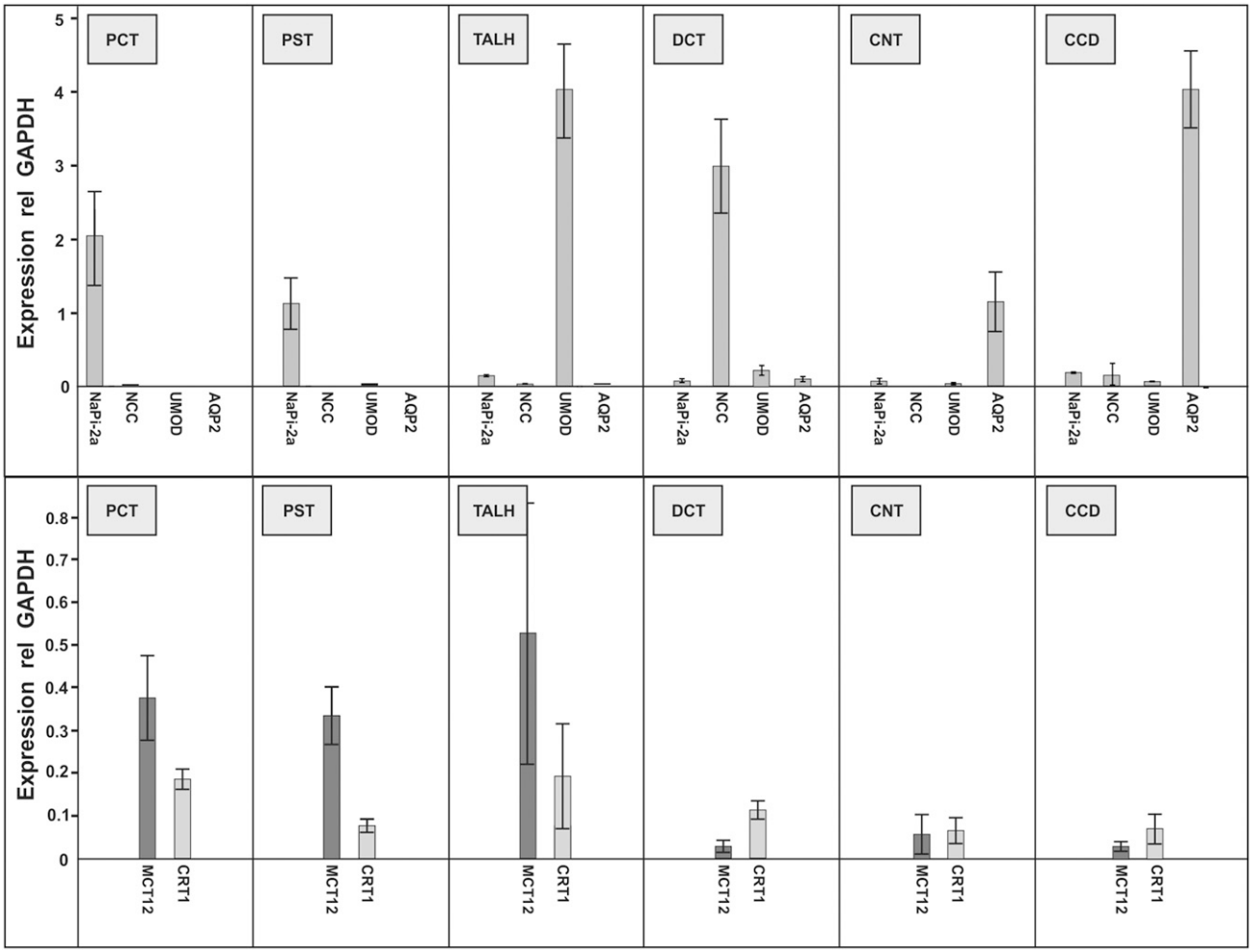

Figure 1. Transcript expression of creatine transporters MCT12 and CRT1 along the mouse nephron. Indicated segments were microdissected, total RNA isolated and reverse transcribed. Expression of indicated transcripts was quantified by Taqman-based RT-PCR and normalized to GAPDH transcript levels. Upper panel: segment-specific transcripts and purity of preparation. Lower panel: expression of MCT12 and CRT1 transcripts. *n*=6 mice; data are means±SD. AQP2, aquaporin-2; CCD, cortical collecting duct; CNT, connecting tubule; DCT, distal convoluted tubule; NaPi-2a, sodium/phosphate cotransporter isoform 2a; NCC, Na- and Cl-cotransporter; PCT, proximal convoluted tubule; PST, proximal straight tubule; TALH, thick ascending limb of loop of Henle; UMOD, uromodulin.

phenotypic characterization included a detailed history, physical examination, and extensive biochemical blood and urine analyses (for details see Concise Methods section and Supplemental Table 1). Given recent insights into MCT12 function, we also specifically determined creatine and its precursor guanidinoacetate in fasting plasma and 24-hour urine samples. Pregnancy in all female subjects was excluded by β-human chorionic gonadotropin testing.

Figure 3 shows an updated version of the original family, including the information obtained during the study.[2] Subjects with microcornea and juvenile cataract are depicted by filled black symbols, presence of normoglycemic glucosuria is highlighted by red frames, and unaffected family members are shown by empty symbols. Family members of generation II and III and their spouses were invited to participate in the study. All participated in the study except individuals II-6, II-12, III-3, and III-9. Individuals of generation IV, with the exception of IV-I, did not undergo blood and urine testing in this study due to their young age.

Two patterns emerged when analyzing plasma and urinary parameters: glucosuria (Table 1) and lower plasma guanidinoacetate levels with increased fractional urinary excretion of guanidinoacetate (Figure 4, Table 2). Glucosuria was present in five of 16 family members tested. In five of these, glucosuria was present in the setting of normoglycemia (fasting glucose $<$5.5 mmol/l) and normal hemoglobin $A1_c$ ($<$6%), and was thus of renal origin. Subject II-9 had significant glucosuria, with a concomitant fasting glucose of 9.3 mmol/l and a hemoglobin $A1_c$ of 7.4%. He was diagnosed with type II diabetes 12 years earlier and treated with metformin and sulfonylurea. Renal leak glucosuria was present in five of 11 patients with the heterozygous *MCT12* mutation. Unlike described in the initial

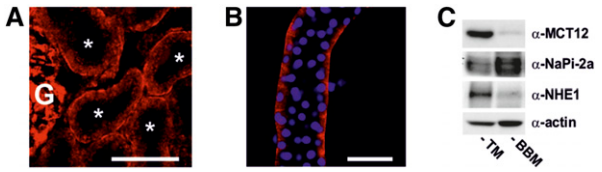

Figure 2. Subcellular localization of MCT12 in mouse kidney. Confocal image of a kidney cryosection (A) and of an isolated proximal convoluted tubule (B) stained with anti-MCT12 antibody. Asterisks indicate proximal tubules. Nuclei were counterstained with DAPI (blue, right panel). White scale bar corresponds to 50 μm. (C) Immunoblot of TM or BBM preparation stained with an anti-MCT12 antibody and a basolateral (NHE1) or apical (NaPi-2a) membrane protein. BBM, brush border membrane; G, Glomerulus; NaPi-2a, sodium/phosphate cotransporter isoform 2a; NHE1, sodium/hydrogen exchanger isoform 1; TM, total kidney membrane preparation.

report, our detailed analysis did not result in finding an individual without *MCT12* mutation that had glucosuria.

Since creatinine is a nonenzymatic degradation product of creatine, GFR estimation based on creatinine may not be reliable in individuals with *MCT12* mutation. We thus also measured plasma cystatin C in all individuals and calculated cystatin-C-based eGFR. Results indicate that GFR is similar in individuals with and without *MCT12* mutation (Table 1), and that there is a good correlation between creatinine and cystatin-C-based GFR estimates in individuals with *MCT12* mutation (Supplemental Figure 2).

To dissect the creatine pathway in more detail, individual plasma and urinary creatine and guanidinoacetate levels were analyzed. As shown in Table 2, comparison of individuals with and without *MCT12* mutation revealed no differences in plasma creatine, but reduced plasma guanidinoacetate in individuals with the *MCT12* mutation ($P<0.01$). The difference in plasma guanidinoacetate remained significant after adjustment for sex, age, body mass index (BMI), and GFR (Table 3). Compared with individuals without the *MCT12* mutation, 24-hour urinary excretions of creatine and guanidinoacetate were higher in patients with the *MCT12* mutation, but the differences did not reach statistical significance, including after adjustment for sex, age, BMI, and GFR (Tables 2 and 3). However, concomitant with a reduced plasma concentration, we observed an increased fractional excretion of guanidinoacetate in individuals with the *MCT12* mutation (Figure 4B), whereas we observed no difference in fractional creatine excretion (Figure 4A). In additional detailed biochemical analyses of blood and urine, with the exception of a mildly reduced 24-hour urinary excretion of the amino acid threonine, we detected no further abnormalities in subjects with the *MCT12* mutation (Supplemental Table 1).

We next tested if human MCT12 is able to transport guanidinoacetate in addition to the already known substrate creatine. For this purpose, untagged human MCT12 was expressed in *Xenopus* oocytes. Two days after injection of oocytes with human MCT12 complementary RNA (cRNA), significant MCT12 protein surface expression (Figure 5A) and creatine transport (Figure 5B) could be observed. As reported previously, H_2O-injected oocytes did not exhibit significant creatine uptake (data not shown).[4] In competition assays, 100 μM guanidinoacetate was used at different concentrations of creatine (Figure 5C). Even at 100-fold excess of guanidinoacetate over creatine, we did not observe an impact of guanidinoacetate on MCT12-mediated creatine transport, clearly indicating that guanidinoacetate is not a substrate for MCT12.

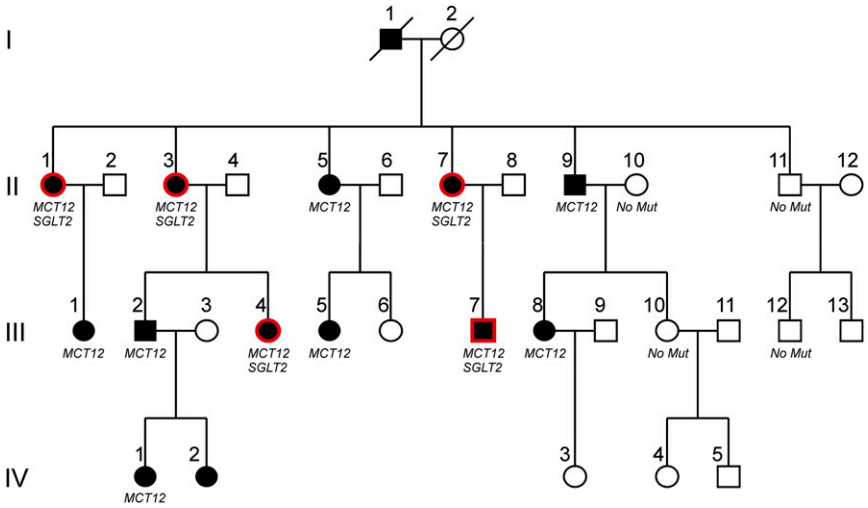

Figure 3. Pedigree of the family with juvenile cataract, microcornea, and glucosuria. Empty symbols indicate absence of cataract and microcornea (all generations). Filled blacked symbols indicate presence of cataract and microcornea. Red frames indicate renal leak glucosuria. For generation I, only anamnestic information was available. For generation IV, only phenotypic eye data were available. Presence or absence of *MCT12* and *SGLT2* mutations is indicated where available. Subjects II-6, II-12, III-3, and III-9 did not participate in this study.

As outlined earlier, the pattern of glucosuria in the family suggested either an MCT12-dependent effect with incomplete penetrance or segregation of an additional genetic disease in the family.[2] Interestingly, family history obtained during this study indicated that the male subject I-1 was suffering from a juvenile cataract, and the female subject I-2 was suffering from glucosuria without diabetes mellitus. Unfortunately, no clinical documentation was available to further substantiate this information. Nevertheless, this additional information prompted us to clearly consider the possibility of a second mutation in the family. Thus, we next sequenced the sodium/glucose cotransporter 2-encoding gene *SGLT2*, coding for the Na^+/glucose cotransporter SGLT2, mutations of which cause

Table 1. Blood and urinary parameters of family members

Individual	*MCT12* Mutation	*SGLT2* Mutation	Age (Years)	Plasma Parameters														24-Hour Urinary Glucose Excretion
				Na	K	Cl	Ca	P	Mg	pH	HCO_3	Glucose	Creatinine	CKD-EPI eGFR	Cystatin C	Cystatin eGFR	Hb $A1_c$	
II-1	yes	yes	70.3	138	4.1	108	2.27	1.12	0.89	7.35	24.3	5.2	67	80	1.07	64	5.6	6.71
II-3	yes	yes	65.3	138	3.8	106	2.22	1.08	0.82	7.39	28.7	4.9	52	96	0.90	82	6.3	11.77
II-7	yes	yes	61.8	139	4.5	102	2.26	0.83	0.83	7.29	25.2	4.5	66	86	0.70	103	5.6	5.54
III-4	yes	yes	40.2	137	3.9	100	2.24	0.85	0.72	7.40	23.5	4.8	66	100	0.53	130	5.7	6.53
III-7	yes	yes	27.1	140	4.8	106	2.25	0.84	0.85	7.34	26.7	5.1	91	99	0.80	119	5.4	1.10
II-5	yes	no	55.3	141	3.9	104	2.27	1.01	0.78	7.43	23.0	4.4	70	98	0.86	90	5.4	0.14
II-9	yes	no	69.4	137	4.3	99	2.38	1.00	0.76	7.36	28.0	9.7	96	69	0.87	90	7.8	32.48
III-1	yes	no	44.8	138	4.2	103	2.31	0.85	0.88	7.39	29.1	4.7	69	92	0.96	81	5.7	0.09
III-2	yes	no	43.3	141	4.1	107	2.29	0.74	0.79	7.37	26.7	4.9	74	107	0.73	117	5.6	0.36
III-5	yes	no	22.4	140	3.6	101	2.24	1.05	0.77	7.37	24.8	3.7	61	106	0.74	118	5.4	0.12
III-8	yes	no	35.6	139	4.4	106	2.15	1.16	0.83	7.39	22.9	4.7	85	76	0.85	99	4.7	0.55
II-2	no	no	68.6	137	4.0	107	2.23	1.06	0.70	7.41	21.7	6.4	73	90	0.90	86	6.9	0.10
II-4	no	no	74.4	142	4.1	102	2.27	1.04	0.80	7.39	26.5	5.4	80	83	0.93	81	6.1	0.27
II-8	no	no	64.7	139	4.4	102	2.22	0.78	0.87	7.36	25.6	4.9	74	92	0.73	107	5.4	0.33
II-10	no	no	70.4	138	4.2	103	2.26	0.96	0.78	7.40	24.6	5.0	63	86	0.74	97	5.7	0.19
II-11	no	no	53.7	136	4.1	101	2.29	0.70	0.77	7.41	23.9	5.4	94	79	0.79	108	5.4	0.39
III-6	no	no	30.5	138	3.9	108	2.20	0.82	0.76	7.37	24.9	5.2	77	89	ND	ND	5.1	0.36
III-10	no	no	38.7	139	4.2	106	2.25	0.96	0.76	7.39	25.3	4.6	74	88	0.69	114	5.1	0.41
III-11	no	no	39.5	143	4.0	105	2.35	0.98	0.89	7.38	27.1	4.7	75	109	0.65	126	5.3	0.64
III-12	no	no	22.6	ND	ND	ND	ND	ND	ND	ND	ND	ND	ND	ND	ND	ND	ND	0.18
III-13	no	no	25.8	140	4.0	102	2.29	1.15	0.88	7.40	25.1	5.1	113	77	0.80	120	5.2	0.18
MCT12 mutation yes, median (IQR)			44.8	139	4.1	104	2.26	1	0.82	7.37	25.2	4.8[a]	69	96 (83–100)	0.85	99 (86–117)	5.6[a]	0.83[a] (0.19–6.3)
			(37.9–63.6)	(138–140)	(3.9–4.4)	(101.5–106)	(2.24–2.28)	(0.85–1.07)	(0.78–0.84)	(7.36–7.39)	(23.9–27.35)	(4.6–4.9)	(66–79.5)		(0.74–0.89)		(5.4–5.7)	
MCT12 mutation no, median (IQR)			46.6	139	4.1	103	2.26	0.96	0.78	7.39	25.1	5.11[a]	75 (74–80)	88 (83–90)	0.77	108 (94–116)	5.4[a]	0.27[a] (0.16–0.38)
			(32.5–67.6)	(138–140)	(4–4.2)	(102–106)	(2.23–2.29)	(0.82–1.04)	(0.76–0.87)	(7.38–7.4)	(24.6–25.6)	(4.9–5.4)			(0.72–0.83)		(5.2–5.7)	
Mann–Whitney *U* test, *P* value			1	0.97	0.82	0.91	0.94	0.57	0.62	0.18	0.62	0.03	0.14	0.41	0.41	0.66	0.46	0.19
SGLT2 mutation yes, median (IQR)			61.8	138	4.1	106	2.25	0.85	0.83	7.35	25.2	4.8[a]	66 (66–67)	96 (86–99)	0.80	105 (82–110)	5.6[a]	6.5[a] (5.5–6.7)
			(40.2–65.3)	(138–139)	(3.9–4.5)	(102–106)	(2.24–2.26)	(0.84–1.08)	(0.82–0.85)	(7.34–7.39)	(24.3–26.7)	(4.8–5.1)			(0.70–0.90)		(5.6–6.5)	
SGLT2 mutation no, median (IQR)			44	139	4.1	103	2.27	0.98	0.78	7.39	25.1	4.9[a]	74	89 (81–95)	0.80	100 (86–109)	5.4[a]	0.27[a] (0.16–0.38)
			(34.3–65.6)	(138–140.5)	(4–4.2)	(102–106)	(2.24–2.29)	(0.84–1.05)	(0.77–0.85)	(7.37–7.4)	(24.25–26.6)	(4.7–5.2)	(71.5–82.5)		(0.70–0.90)		(5.2–5.7)	
Mann–Whitney *U* test, *P* value			0.60	0.43	0.79	0.69	0.36	0.93	0.41	0.13	0.79	1.00	0.09	0.55	1	0.89	0.16	0.001

Numbering is according to the pedigree in Figure 1. Raw data, median, and interquartile range (IQR) of all parameters are presented. Between-group differences were analyzed by the Mann–Whitney *U* test. Plasma Na, K, Cl, P, Mg, HCO_3, and glucose are in mmol/l, and plasma creatinine in μmol/l. Glucose excretion per 24 hours in the urine is in mmol. CKD-EPI, Chronic Kidney Disease Epidemiology Collaboration; $HbA1_c$, glycated hemoglobin; ND, not determined.

[a]Subject II-9 suffers from diabetes mellitus type II. He was therefore excluded from the statistical analyses concerning the comparison between patients with and without the *SGLT2* mutation for the following parameters: plasma glucose, $HbA1_c$, and glucose excretion per 24 hours.

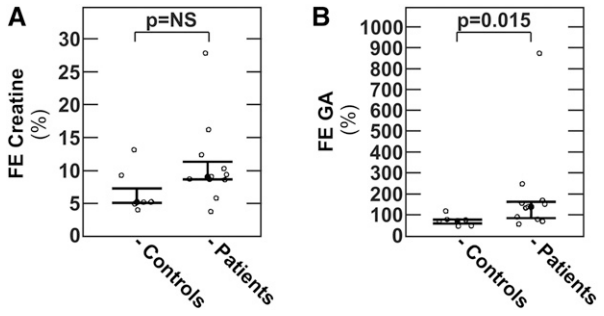

Figure 4. Fractional excretion of creatine and guanidinoacetate in individuals with and without the heterozygous p.Q215× *MCT12* mutation. Fractional excretion of (A) creatine or (B) guanidinoacetate in individuals with (patients) and without (controls) *MCT12* mutation. Fractional excretions were calculated using cystatin-C-based GFR estimates. Data are medians with interquartile range. FE, fractional excretion; NS, nonsignificant.

isolated renal glucosuria.[11] Sequence analysis revealed a novel, hitherto undescribed heterozygous c.265G>A; p.A89T mutation of *SGLT2* in the family. As shown in Figure 3 and Table 1, with the sole exception of subject II-9 with poorly controlled diabetes mellitus, we observed complete cosegregation of the glucosuria trait with this novel *SGLT2* mutation.

To confirm that the p.A89T transition in SGLT2 was indeed pathogenic, we conducted *in vitro* experiments with wild-type and mutant SGLT2 constructs. For this, mutant p.A89T and wild-type SGLT2 were expressed in HEK293 cells, and total and plasmalemmal expression was analyzed. As shown in Figure 6A when analyzing whole cell lysates (input) by SDS-PAGE and immunoblotting, wild-type SGLT2 migrated as a prominent 60 kDa and a weak 50 kDa band. In contrast, mutant SGLT2 gave rise to a strong 50 kDa band and a faint 60 kDa band. Furthermore, surface biotinylation experiments demonstrated that mutant SGLT2 had greatly reduced plasma membrane expression (Figure 6A). Of the wild-type protein, only the 60 kDa, but not the 50 kDa form was present on the cell surface, indicating that the 60 kDa is the mature form of the transporter destined for the plasma membrane. Compatible with reduced plasmalemmal expression, functional analysis revealed significantly reduced [^{14}C]-α-methyl-D-glucopyranoside ([^{14}C]-α-MDG) uptake in HEK293 cells transfected with the mutant SGLT2 construct (Figure 6B). Next, we investigated if the observed size shift of the mutant

Table 2. Plasma and urinary creatine and guanidinoacetate levels of family members

Individual	*MCT12* Mutation	*SGLT2* Mutation	Age (Years)	Plasma		24-Hour Urine	
				Creatine	Guanidinoacetate	Creatine	Guanidinoacetate
II-1	yes	yes	70.3	26.1	2.02	252	167
II-3	yes	yes	65.3	41.4	3.23	1512	656
II-7	yes	yes	61.8	23.3	0.72	359	312
III-4	yes	yes	40.2	39.6	2.21	300	342
III-7	yes	yes	27.1	28.6	1.97	597	573
II-5	yes	no	55.3	27.7	2.04	421	474
II-9	yes	no	69.4	48.0	2.10	480	242
III-1	yes	no	44.8	43.3	1.62	430	100
III-2	yes	no	43.3	31.4	0.67	576	1256
III-5	yes	no	22.4	29.0	2.40	926	710
III-8	yes	no	35.6	24.0	2.20	428	531
II-2	no	no	68.6	51.0	3.50	371	226
II-4	no	no	74.4	57.0	3.70	380	222
II-8	no	no	64.7	9.6	2.18	205	244
II-10	no	no	70.4	47.0	3.70	583	368
II-11	no	no	53.7	44.0	2.40	343	354
III-6	no	no	30.5	26.0	2.40	229	186
III-10	no	no	38.7	34.0	3.20	297	630
III-11	no	no	39.5	26.2	3.51	324	556
III-12	no	no	22.6	23.0	2.10	261	91
III-13	no	no	25.8	ND	ND	932	661
MCT12 mutation yes, median (IQR)			44.8 (37.9–63.6)	29.0 (26.9–40.5)	2.04 (1.80–2.21)	430 (390–586)	474 (277–614)
MCT12 mutation no, median (IQR)			46.6 (32.5–67.6)	34.0 (26.0–47.0)	3.20 (2.40–3.50)	333 (270–378)	299 (223–509)
Mann–Whitney *U* test, *P* value			1	0.77	<0.01	0.09	0.43
SGLT2 mutation yes, median (IQR)			61.8 (40.2–65.3)	28.6 (26.1–39.6)	2.02 (1.97–2.21)	359 (300–597)	342 (312–573)
SGLT2 mutation no, median (IQR)			44 (34.3–65.6)	31.4 (26.1–45.5)	2.40 (2.10–3.40)	400 (317–504)	361 (225–575)
Mann-Whitney *U* test, *P* value			0.60	0.55	0.20	0.90	0.97

Numbering is according to the pedigree in Figure 1. Raw data as well as median and interquartile range (IQR) of all parameters are presented. Between-group differences were analyzed by the Mann–Whitney *U* test. Plasma creatine and guanidinoacetate are in μmol/l. Creatine and guanidinoacetate excretion in the 24-hour urine are in μmol/24 h.

Table 3. Associations between the *MCT12* mutation and plasma and urinary creatine and guanidinoacetate by linear regression models

Response Variable	Model 1				Model 2				Model 3			
	β	95% CI	*P* Value	R^2	β	95% CI	*P* Value	R^2	β	95% CI	*P* Value	R^2
Plasma creatine	−2.37	(−13.82 to 9.08)	0.67	−0.04	−3.90	(−15.32 to 11.53)	0.77	<−0.004	−6.03	(−24.17 to 12.12)	0.48	−0.13
Plasma guanidinoacetate	−1.04	(−1.71 to −0.37)	0.0042	0.34	−1.19	(−2.01 to −0.37)	0.0074	0.30	−1.66	(−2.68 to −0.64)	0.0041	0.38
Creatine in 24-hour urine	178	(−97 to 104)	0.19	0.04	220	(−123 to 564)	0.19	−0.04	163	(−315 to 640)	0.47	−0.22
Guanidinoacetate in 24-hour urine	134	(−114 to 382)	0.27	0.01	184	(−130 to 499)	0.23	−0.03	130	(−240 to 501)	0.46	0.078

Model 1: univariate association. Model 2: adjusted for sex, age, and body mass index. Model 3: as Model 2 plus adjusted for cystatin C eGFR. The β coefficient of the prediction variable *MCT12* mutation is indicated. *MCT12* has the wild-type as reference group. The adjusted R-squared (R^2) has been adjusted for all predictors in the model. Plasma creatine and guanidinoacetate are in μmol/l. Creatine and guanidinoacetate excretion in the 24-hour urine are in μmol/24 h. 95% CI, 95% confidence interval.

SGLT2 compared with wild-type SGLT2 was due to impaired N-linked glycosylation. For this, lysates of HKE293 cells transfected with wild-type and mutant SGLT2 constructs were treated with PNGase F to remove N-linked glycosylation. As shown in Figure 6C, after treatment with PNGase F, both wild-type and mutant SGLT2 migrated as a single band at 50 kDa, indicating a lack of N-glycosylation in mutant SGLT2.

DISCUSSION

The creatine transporter MCT12 has been shown to be involved in the pathogenesis of juvenile cataracts in humans.[2] Based on the mRNA expression pattern, an additional function of MCT12 in the kidney has been previously suspected.[2,3] Here, we show that the MCT12 transcript is expressed in both proximal tubules and the thick ascending limbs of the loop of Henle, and our localization studies indicate that MCT12 resides on the basolateral membrane. In contrast, CRT1 was reported to be a brush border protein.[12] Our findings of basolateral MCT12 localization in the kidney are consistent with the basolateral localization reported for CD147, which is an accessory protein for several monocarboxylate transporters of the SLC16 family transporters, including MCT12.[3]

Individuals with *MCT12* mutation displayed unaltered fractional excretion of creatine, but increased fractional excretion of guanidinoacetate. In seven of 11 individuals with *MCT12* mutation, the fractional excretion of guanidinoacetate significantly exceeded 100%, indicating glomerular filtration

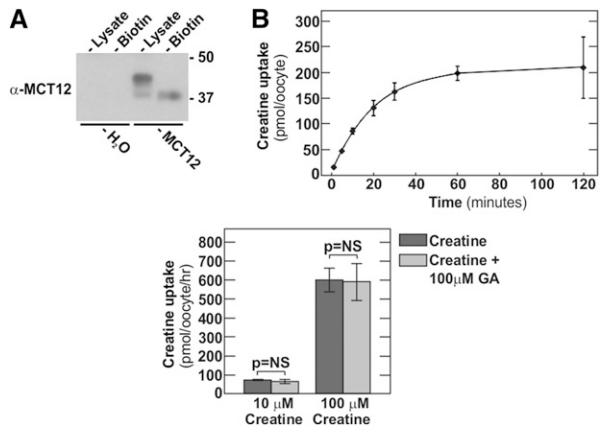

Figure 5. Human MCT12 does not transport guanidinoacetate. Transport assay in *Xenopus* oocytes. (A) Immunoblot of cell lysates or surface biotin fractions of *Xenopus* oocytes 2 days after injection with (untagged) human MCT12 cRNA or H_2O only. (B) Time course of MCT12-mediated creatine uptake at 100 μM creatine concentration 2 days after injection. (C) Competition of MCT12-mediated creatine uptake at 1 μM creatine (left panel) or 10 and 100 μM creatine (right panel), with or without 100 μM guanidinoacetate (GA) 2 days after injection. Data are means±SD.

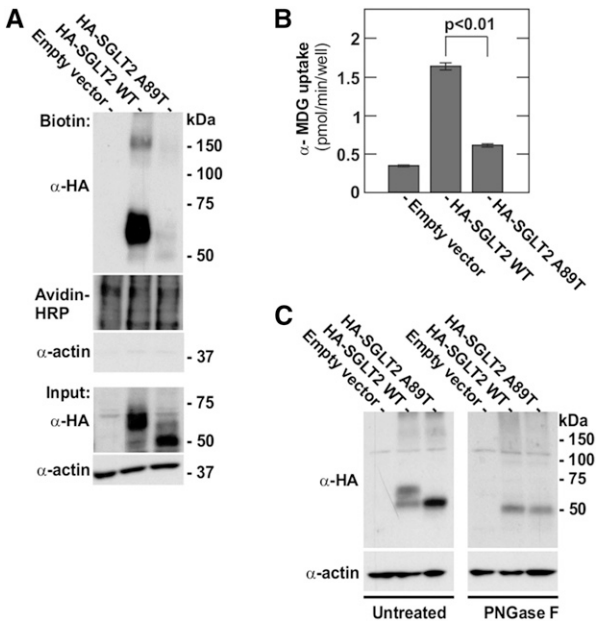

Figure 6. Reduced SGLT2 A89T membrane expression and transport activity. (A) Plasma membrane expression of human SGLT2 wild-type and SGLT2 A89T mutant constructs expressed in HEK293 cells was assessed by immunoblotting of plasma membrane proteins labeled by sulfo-NHS-LC-biotin and isolated with streptavidin agarose beads. Avidin–horseradish peroxidase was used as loading control for surface proteins. The absence of an actin signal confirms the purity of the membrane fraction. (B) Uptake of 50 μM [^{14}C]-α-MDG by HEK293 cells transfected by the indicated constructs. Data are means±SD. (C) Deglycosylation experiment: 20 μg of total protein isolated from HEK cells transfected by the indicated constructs were treated (right panel) or not (left panel) by PNGase F. Actin was used as a loading control.

and secretion of guanidinoacetate. At the moment, especially in the absence of functional data on guanidinoacetate handling in MCT12-deficient rodents, it is not clear how these findings can be reconciled with the fact that MCT12 does not transport guanidinoacetate. Although we did not observe signs of a generalized proximal tubular dysfunction (Fanconi syndrome), the most likely explanation is that the *MCT12* mutation exerts a dominant-negative effect causing proximal tubular dysfunction, similar to what was proposed for the eye.[3]

We did not detect altered plasma levels or renal handling of creatine in subjects with the *MCT12* mutation. This finding is in agreement with observations in *mct12* heterozygous rats.[4] Whereas KO rats exhibit increased excretion of creatine in the urine, heterozygous rats have urinary excretion of creatine that is identical to wild-type animals. Plasma creatine and guanidinoacetate levels, and urinary guanidinoacetate excretion have not been determined in these transgenic rats. Thus, the exact contribution of MCT12 to overall creatine and guanidinoacetate homeostasis remains unknown. Additional studies, including a detailed analysis of renal guanidinoacetate and creatine handling in *mct12* KO rats, will be needed to answer this question.

In addition to new insights into guanidinoacetate homeostasis in humans, our study also offers an explanation for the puzzling observation of glucosuria in the family, which was difficult to reconcile with the known functional properties of MCT12. Our genetic analysis, as well as *in vitro* experiments clearly indicate that the glucosuria observed in the family is caused by cosegregation of a separate, hitherto undescribed heterozygous *SGLT2* mutation, and not by the *MCT12* mutation. Homozygous, compound heterozygous, and heterozygous mutations in *SGLT2* are known to cause renal glucosuria.[11] Typically, glucosuria is more severe in the homozygous or compound heterozygous state (>10 g glucose per day) and milder in heterozygous individuals (<10 g glucose per day). The exclusion of glucosuria as part of the *MCT12* mutation syndrome is clinically relevant. The differential diagnosis of congenital renal glucosuria is narrow, and a *MCT12* mutation has been part of this differential diagnosis since the initial description of the family.[1]

In summary, our study of the only family with a mutation in *MCT12* described thus far indicates that MCT12 plays an important role in whole body homeostasis and renal handling of the creatine precursor guanidinoacetate. However, our data argue strongly against a role for MCT12 in renal glucose transport.

CONCISE METHODS

Family Members and Study Protocol

Family members were studied at the Division of Nephrology, Hypertension and Clinical Pharmacology at the University Hospital of Bern, Switzerland. All participants provided written informed consent and the study was approved by the ethical committee of the Kanton Bern, Switzerland (Approval 129/13).

Blood and Urine Biochemistry

With the exception of creatine and guanidinoacetate, urine and blood analysis was performed by the Central Laboratory of the University Hospital of Bern, Switzerland using standard laboratory methods. Blood-gas analysis was done on venous blood samples. eGFR was calculated from plasma creatinine according to the Chronic Kidney Disease Epidemiology Collaboration formula[13] or from plasma cystatin C.[14] Body surface area (BSA) was estimated using the Dubois formula: BSA (m^2)=0.202476×height (m)$^{0.7256}$×weight (kg)$^{0.425}$. Determination of creatine and guanidinoacetate was performed at the Division of Clinical Chemistry and Biochemistry, University Children's Hospital, Zürich, Switzerland. Creatine and guanidinoacetate in plasma and urine were determined as butyl esters by liquid chromatography-electrospray ionization tandem mass-spectrometry, based on descriptions by Bodamer *et al.* and Cognat *et al.*[15,16] A SCIEX 4000 QTrap instrument was used and multiple reaction monitoring was applied for the detection of the following ion transitions: analytes (174.1>101.0 for guanidinoacetic acid and 188.1>89.95 for creatine) and internal standards (176.1>103.0 for guanidinoacetic-2,2-d_2 acid and 191.0>93.0 for creatine-d_3 [methyl-d_3]).

DNA Extraction and Genotyping

Genomic DNA was prepared from peripheral blood leukocytes by magnetic bead technology (Chemagen).[17] Exons with adjacent exon-intron boundaries of the *MCT12* and *SGLT2* genes were individually amplified by PCR (AmpliTaq Gold system, Applied Biosystems) and the DNA sequence of both strands was determined by bidirectional Sanger sequencing. *MCT12* primers were described previously.[2,11] Sequencing primers for *SGLT2* are detailed in Supplemental Material.

Generation and Subcloning of Human SGLT2 Constructs

The clone Hu14 containing the human SGLT2 cDNA isolated from the human kidney cDNA library was used as a template.[18] An N-terminal HA tag was added by PCR and then subcloned into the vector pcDNA3.1. This construct was then used as a template for the site-directed mutagenesis by the QuickChange site-directed mutagenesis kit (Agilent Technologies) to generate the human G265A mutation, corresponding to an A89T substitution in human SGLT2.

Cell Culture and Transfection

HEK293 cells were obtained from the American Type Culture Collection and maintained in high glucose DMEM (Invitrogen) supplemented with 10% non-heat inactivated FBS (Invitrogen), 100 U/ml penicillin, and 100 U/ml streptomycin, and grown in a humidified 95%/5% air/CO_2 atmosphere incubator at 37°C. cDNA transfections were performed with Lipofectamine 2000 (Invitrogen), according to manufacturer's instructions.

Deglycosylation Experiments

1×10^6 HEK293 cells were seeded on six-well plates and transfected with the different constructs. The next day, cells were washed two times with PBS and lysed in lysis buffer (150 mM NaCl, 5 mM EDTA, 1% NP40, 0.5% sodium deoxycholate, and 50 mM Tris, pH 7.4). Then, 20 μg of protein were digested for 24 hours at 37°C with 4 μl PNGase F (New England BioLabs) in reaction buffer (50 mM sodium phosphate buffer, pH 7.5). Digestions were terminated by addition of 8 μl 4× Lämmli buffer. Samples were then separated by SDS-PAGE and analyzed by immunoblotting.

Surface Biotinylation and Immunoblotting

Surface biotinylation was conducted as previously described.[19] Cells were rinsed three times with PBS, then surface proteins were biotinylated by incubating cells with 1.5 mg/ml sulfo-NHS-LC-biotin in 10 mM triethanolamine (pH 7.4), 1 mM $MgCl_2$, 2 mM $CaCl_2$, and 150 mM NaCl for 90 minutes, with horizontal motion at 4°C. After labeling, cells were washed with quenching buffer (PBS containing 1 mM $MgCl_2$, 0.1 mM $CaCl_2$, and 100 mM glycine) for 20 minutes at 4°C, and then rinsed once with ice-cold PBS. Cells were then lysed in radioimmunoprecipitation (RIPA) buffer (150 mM NaCl, 50 mM Tris·HCl [pH 7.4], 5 mM EDTA, 1% Triton X-100, 0.5% deoxycholate, and 0.1% SDS) and lysates were cleared by centrifugation. Cell lysates of equivalent amounts of protein were equilibrated overnight with streptavidin agarose beads at 4°C. Beads were washed sequentially with solution A (50 mM Tris·HCl [pH 7.4], 100 mM NaCl, and 5 mM EDTA) three times, solution B (50 mM Tris·HCl [pH 7.4], and 500 mM NaCl) two times, and solution C (50 mM Tris·HCl, pH 7.4) once. Biotinylated proteins were then released by heating to 95°C with 2.5× Lämmli buffer, and separated by SDS-PAGE.

For surface biotinylation of oocytes, oocytes were incubated for 1 hour at 4°C in PBS containing 1.5 mg/ml sulfo-LC-NHS-(+)-Biotin (Pierce), washed three times with quenching solution (PBS containing 100 mM glycine), and lysed in 1 ml RIPA buffer on a rocker for 2 hours at 4°C. Then, lysates were centrifuged at 20,000*g* for 15 minutes at 4°C and supernatants were transferred into new tubes. Biotinylated proteins were isolated by addition of 50 μl of streptavidin agarose beads (Pierce), overnight incubation at 4°C, and recovery of the beads by centrifugation at 9,000*g* (1 minute at 4°C). Beads were washed three times with RIPA buffer and proteins were released from the beads by boiling in 2× Lämmli buffer.

For immunoblotting, monoclonal anti-HA antibody (1:1000 dilution, Sigma-Aldrich) was used followed by a secondary horseradish peroxidase–conjugated goat anti-mouse antibody (1:3000 dilution, Bio-Rad Laboratories). Signals were detected by enhanced chemiluminescence (GE Healthcare). Polyclonal anti-actin was from Santa Cruz Biotechnology and avidin–secondary horseradish peroxidase was from Bio-Rad Laboratories.

[^{14}C]-α-Methyl-D-Glucopyranoside Uptake in HEK Cells

A total of 180,000 HEK293 cells were seeded in 24-well plates. The next day, cells were transfected with empty vector, SGLT2 wild-type, or mutant A89T SLGT2. At 24 hours after transfection, cells were washed twice with 1 ml of choline buffer (150 mM choline chloride, 2 mM KCl, 1 mM$CaCl_2$, 1 mM $MgCl_2$, and 10 mM HEPES, pH 7.4) and incubated for 5 minutes in the same buffer at 37°C. Then, the solution was replaced by 250 μl uptake solution (same composition as the choline buffer except that choline chloride was replaced by an equimolar concentration of NaCl) containing 50 μM [14C]-α-methyl-D-glucopyranoside (α-MDG) including 0.25 μCi [^{14}C]-α-MDG. Uptake was carried out for 30 minutes at 37°C and was stopped by washing the cells three times with 1 ml of ice-cold choline buffer containing 10 mM α-MDG. Cells were then lysed in 500 μl of 5% SDS for 1 hour and transferred into scintillation vials. Then, 3 ml of scintillation fluid was added into each vial and uptaken [^{14}C]-α-MDG was detected with the TRI-CARB 2100TR Liquid Scintillation Analyzer (Packard).

Tubule Microdissection, RNA Isolation, and RT-PCR

Tubules were microdissected from male C57BL6/J mice that had free access to tap water and standard laboratory chow. After deep anesthesia, kidneys were perfused with 40 μg/ml Liberase Blendzyme 2 (Roche Applied Science) dissolved in DMEM/F-12 (Invitrogen). Thin pyramids cut along the corticomedullary axis were further incubated at 37°C for 40 minutes in the same medium. Microdissection was performed in ice-cold DMEM/F-12 (1:1) as described.[20] The following structures were isolated: glomeruli, convoluted and straight proximal tubules, medullary and cortical portions of the thick ascending limb, distal convoluted and connecting tubules, and cortical portions of the collecting ducts. RNA was isolated from microdissected tubules using an RNeasy micro Kit (Qiagen), following the manufacturer's instructions. Reverse transcription was performed using the Taqman Reverse Transcription kit (Life

Technologies/ABI). RT-PCR was performed using presynthesized Taqman-based Assays-on-Demand (Life Technologies/ABI) on an ABI ViiA 7 System. The following assays-on-demand were employed: NaPi-2a (Mm00441450_m1), Uromodulin (Mm00447649_m1), NCC (Mm00490213_m1), AQP2 (Mm00437575_m1), MCT12 (Mm00556020_m1), CRT1 (Mm00506023_m1), and GAPDH (Mm99999915_g1). Ct values for triplicate technical replicates were averaged and the amount of mRNA relative to GAPDH was calculated using the ΔCt method.

Immunofluorescence and Confocal Microscopy

Kidneys of anesthetized adult mice were fixed by vascular perfusion with 3% paraformaldehyde and processed for immunohistochemistry exactly as described.[21] Cryosections were incubated with the previously validated polyclonal rabbit anti-MCT12 (1:200) antibody,[3] followed by an Alexa 568-conjugated secondary antibody (Invitrogen). All antibodies dilutions were in PBS/1.5% BSA. Images were obtained through a Nikon C1 confocal microscope.

Preparation of Brush Border Membrane Vesicles and Total Membrane Fractions

Renal cortical brush border membrane vesicles (BBMV) were prepared by the Mg^{2+} aggregation method as previously described.[22] Briefly, fresh kidney cortical samples were homogenized in ice-cold isolation buffer (300 mM Mannitol, 5 mM EGTA, and 18 mM HEPES with pH adjusted to 7.5 with a 1M Tris base) containing fresh protease inhibitors, and crude membranes were obtained by centrifugation at 48,000*g* for 1 hour at 2°C. Pellets were resuspended, homogenized in a Dounce glass homogenizer, and subjected to Mg^{2+} aggregation by addition of $MgCl_2$ to a final concentration of 15 mM at 4°C for 20 minutes. Aggregated membranes were removed by centrifugation at 3000*g* for 10 minutes at 2°C, and the supernatant was subjected to two additional rounds of Mg^{2+} aggregation as above, followed by centrifugation at 48,000*g* for 30 minutes at 2°C. The resulting pellet enriched in BBMV was dissolved in 200 μl ice-cold RIPA buffer.

Total membrane fractions were prepared from frozen kidneys after homogenization in freshly made membrane preparation buffer (200 mM mannitol, 80 mM HEPES, 41 mM KOH, and one dissolved Complete Protease Inhibitor tablet [Roche Diagnostics]) using a homogenizer. The homogenate was then centrifuged for 15 minutes at 4°C and 2,600*g*, and the resulting supernatant was placed in an ultracentrifuge (Beckman ultracentrifuge tubes) for 1 hour at 100,000*g* and 4°C. The pellet was resuspended in resuspension buffer, and protein concentration was quantified using a colorimetric assay (DcProtein Assay, Bio-Rad Laboratories). A total of 40 μg of dissolved BBMV protein or total kidney membrane protein were then used for separation by SDS-PAGE.

Functional Studies of Human MCT12 in *Xenopus* Oocytes

Ovarian tissue was surgically removed from the frogs and treated with 2 mg/ml of collagenase NB4 (Serva) for 2 hours in Modified Barth Medium (MBM; 88 mM NaCl, 1 mM KCl, 2.4 mM $NaHCO_3$, 0.82 mM $MgSO_4$, 0.66 mM $NaNO_3$, 0.75 mM $CaCl_2$, 10 mM HEPES-NaOH, pH 7.5) without $CaCl_2$ and supplemented with 50 μg/ml gentamicin. Subsequently, defolliculated stage V-VI oocytes were isolated, transferred into plates containing MBM medium supplemented with gentamicin, and maintained at 18°C prior to injection. Depending on the experiment, oocytes were injected with 40 ng of cDNA-derived cRNA (*in-vitro* transcription with the mMESSAGE mMACHINE T3 kit, Ambion).[4] For injection, a Nanoinject II microinjector (Drummond) was used. Injection volume was 56 nl. A minimum of five oocytes were injected for each experimental condition.

Transport studies were performed at day 2 after injection. For uptake experiments, 0.2 μCi C_{14}-radiolabeled creatine (Hartmann Analytic) and indicated cold amounts of creatine and guanidinoacetate were used. After 10 minutes, uptake was stopped by removing the uptake solution and washing the oocytes extensively with ND100 (100 mM NaCl, 2 mM KCl, 1 mM $CaCl_2$, 10 mM Hepes-NaOH, pH 7.5). Radioactivity was measured by liquid scintillation counting (scintillation solution: Igrasafe plus [Zinsser Analytic], scintillation counter: Tri-Carb 2100TR [Packard]).

Statistical Analyses

Blood and urinary parameters were presented as raw data, median, and interquartile range, and were compared by Mann–Whitney *U* tests, according to the presence or absence of *MCT12* and *SGLT2* mutation, respectively. All statistical tests were two-sided and a P value <0.05 was considered to indicate a statistically significant difference. In order to estimate the associations between the *MCT12* mutation and plasma and urinary creatine and guanidinoacetate levels, we first applied univariable linear regression analyses in model one. To analyze the independent associations of the *MCT12* mutation with the response variables of interest, multilevel multivariable regression analyses were conducted adjusting for sex, age, and BMI in model two, and then additionally for cystatin-C-based estimation of GFR in model three. Statistical analyses were performed using the R Statistics software version 3.0.2.[23]

ACKNOWLEDGMENTS

We thank Nancy Philp for the generous gift of the MCT12 antibody and Silvio Tedaldi, Christine Hohl, and David Wenner for technical assistance.

D.F. was supported by the Swiss National Centres of Competence in Research TransCure, the Swiss National Science Foundation (grants No. 31003A_135503 and 31003A_152829) and by a Medical Research Position Award of the Foundation Prof. Dr. Max Cloëtta.

DISCLOSURES

D.F. has served on an advisory board for Otsuka Pharmaceuticals and received unrestricted research grants from Novartis and Abbvie.

REFERENCES

1. Vandekerckhove K, Lange AP, Herzog D, Schipper I: [Juvenile cataract associated with microcornea and glucosuria: a new syndrome]. *Klin Monbl Augenheilkd* 224: 344–346, 2007

2. Kloeckener-Gruissem B, Vandekerckhove K, Nürnberg G, Neidhardt J, Zeitz C, Nürnberg P, Schipper I, Berger W: Mutation of solute carrier SLC16A12 associates with a syndrome combining juvenile cataract with microcornea and renal glucosuria. *Am J Hum Genet* 82: 772–779, 2008
3. Castorino JJ, Gallagher-Colombo SM, Levin AV, Fitzgerald PG, Polishook J, Kloeckener-Gruissem B, Ostertag E, Philp NJ: Juvenile cataract-associated mutation of solute carrier SLC16A12 impairs trafficking of the protein to the plasma membrane. *Invest Ophthalmol Vis Sci* 52: 6774–6784, 2011
4. Abplanalp J, Laczko E, Philp NJ, Neidhardt J, Zuercher J, Braun P, Schorderet DF, Munier FL, Verrey F, Berger W, Camargo SM, Kloeckener-Gruissem B: The cataract and glucosuria associated monocarboxylate transporter MCT12 is a new creatine transporter. *Hum Mol Genet* 22: 3218–3226, 2013
5. Wyss M, Kaddurah-Daouk R: Creatine and creatinine metabolism. *Physiol Rev* 80: 1107–1213, 2000
6. Takeda M, Kiyatake I, Koide H, Jung KY, Endou H: Biosynthesis of guanidinoacetic acid in isolated renal tubules. *Eur J Clin Chem Clin Biochem* 30: 325–331, 1992
7. Takeda M, Koide H, Jung KY, Endou H: Intranephron distribution of glycine-amidinotransferase activity in rats. *Ren Physiol Biochem* 15: 113–118, 1992
8. Van Pilsum JF, Stephens GC, Taylor D: Distribution of creatine, guanidinoacetate and enzymes for their biosynthesis in the animal kingdom. Implications for phylogeny. *Biochem J* 126: 325–345, 1972
9. van de Kamp JM, Betsalel OT, Mercimek-Mahmutoglu S, Abulhoul L, Grünewald S, Anselm I, Azzouz H, Bratkovic D, de Brouwer A, Hamel B, Kleefstra T, Yntema H, Campistol J, Vilaseca MA, Cheillan D, D'Hooghe M, Diogo L, Garcia P, Valongo C, Fonseca M, Frints S, Wilcken B, von der Haar S, Meijers-Heijboer HE, Hofstede F, Johnson D, Kant SG, Lion-Francois L, Pitelet G, Longo N, Maat-Kievit JA, Monteiro JP, Munnich A, Muntau AC, Nassogne MC, Osaka H, Ounap K, Pinard JM, Quijano-Roy S, Poggenburg I, Poplawski N, Abdul-Rahman O, Ribes A, Arias A, Yaplito-Lee J, Schulze A, Schwartz CE, Schwenger S, Soares G, Sznajer Y, Valayannopoulos V, Van Esch H, Waltz S, Wamelink MM, Pouwels PJ, Errami A, van der Knaap MS, Jakobs C, Mancini GM, Salomons GS: Phenotype and genotype in 101 males with X-linked creatine transporter deficiency. *J Med Genet* 50: 463–472, 2013
10. Salomons GS, van Dooren SJ, Verhoeven NM, Cecil KM, Ball WS, Degrauw TJ, Jakobs C: X-linked creatine-transporter gene (SLC6A8) defect: a new creatine-deficiency syndrome. *Am J Hum Genet* 68: 1497–1500, 2001
11. Santer R, Kinner M, Lassen CL, Schneppenheim R, Eggert P, Bald M, Brodehl J, Daschner M, Ehrich JH, Kemper M, Li Volti S, Neuhaus T, Skovby F, Swift PG, Schaub J, Klaerke D: Molecular analysis of the SGLT2 gene in patients with renal glucosuria. *J Am Soc Nephrol* 14: 2873–2882, 2003
12. Li H, Thali RF, Smolak C, Gong F, Alzamora R, Wallimann T, Scholz R, Pastor-Soler NM, Neumann D, Hallows KR: Regulation of the creatine transporter by AMP-activated protein kinase in kidney epithelial cells. *Am J Physiol Renal Physiol* 299: F167–F177, 2010
13. Levey AS, Stevens LA, Schmid CH, Zhang YL, Castro AF 3rd, Feldman HI, Kusek JW, Eggers P, Van Lente F, Greene T, Coresh J; CKD-EPI (Chronic Kidney Disease Epidemiology Collaboration): A new equation to estimate glomerular filtration rate. *Ann Intern Med* 150: 604–612, 2009
14. Inker LA, Schmid CH, Tighiouart H, Eckfeldt JH, Feldman HI, Greene T, Kusek JW, Manzi J, Van Lente F, Zhang YL, Coresh J, Levey AS; CKD-EPI Investigators: Estimating glomerular filtration rate from serum creatinine and cystatin C. *N Engl J Med* 367: 20–29, 2012
15. Bodamer OA, Bloesch SM, Gregg AR, Stockler-Ipsiroglu S, O'Brien WE: Analysis of guanidinoacetate and creatine by isotope dilution electrospray tandem mass spectrometry. *Clin Chim Acta* 308: 173–178, 2001
16. Cognat S, Cheillan D, Piraud M, Roos B, Jakobs C, Vianey-Saban C: Determination of guanidinoacetate and creatine in urine and plasma by liquid chromatography-tandem mass spectrometry. *Clin Chem* 50: 1459–1461, 2004
17. Zuercher J, Neidhardt J, Magyar I, Labs S, Moore AT, Tanner FC, Waseem N, Schorderet DF, Munier FL, Bhattacharya S, Berger W, Kloeckener-Gruissem B: Alterations of the 5'untranslated region of SLC16A12 lead to age-related cataract. *Invest Ophthalmol Vis Sci* 51: 3354–3361, 2010
18. Wells RG, Pajor AM, Kanai Y, Turk E, Wright EM, Hediger MA: Cloning of a human kidney cDNA with similarity to the sodium-glucose cotransporter. *Am J Physiol* 263: F459–F465, 1992
19. Simonin A, Fuster D: Nedd4-1 and beta-arrestin-1 are key regulators of Na+/H+ exchanger 1 ubiquitylation, endocytosis, and function. *J Biol Chem* 285: 38293–38303, 2010
20. Michlig S, Mercier A, Doucet A, Schild L, Horisberger JD, Rossier BC, Firsov D: ERK1/2 controls Na,K-ATPase activity and transepithelial sodium transport in the principal cell of the cortical collecting duct of the mouse kidney. *J Biol Chem* 279: 51002–51012, 2004
21. Loffing J, Loffing-Cueni D, Valderrabano V, Kläusli L, Hebert SC, Rossier BC, Hoenderop JG, Bindels RJ, Kaissling B: Distribution of transcellular calcium and sodium transport pathways along mouse distal nephron. *Am J Physiol Renal Physiol* 281: F1021–F1027, 2001
22. Booth AG, Kenny AJ: A rapid method for the preparation of microvilli from rabbit kidney. *Biochem J* 142: 575–581, 1974
23. R Development Core Team (2008). R: A language and environment for statistical computing. R Foundation for Statistical Computing, Vienna, Austria. ISBN 3-900051-07-0, URL http://www.R-project.org

This article contains supplemental material online at http://jasn.asnjournals.org/lookup/suppl/doi:10.1681/ASN.2015040411/-/DCSupplemental